






# The Investigation of Forward and Backward Brillouin Scattering in High- $Q$ Chalcogenide Microspheres

Jibo Yu , Zhen Shen, Zhiyong Yang , Sisheng Qi, Yuxuan Jiang, Gilberto Brambilla ,  
Chun-Hua Dong , and Pengfei Wang 

**Abstract**—Traditional optomechanical research is rarely studied in compound glass, especially chalcogenide glass. In this paper, the forward and backward Stimulated Brillouin Scattering (SBS) is demonstrated for the first time in a chalcogenide glass microsphere resonator. A high-purity chalcogenide glass microsphere with a high quality ( $Q$ ) factor of  $2.1 \times 10^7$  is investigated using a 1550 nm tunable laser. In the experiment, the resulting mechanical vibration frequencies caused by forward and backward SBS are measured at 80 MHz and 7.8 GHz, respectively. The triply resonant Stimulated Brillouin scattering process greatly enhances the light–acoustic interactions, enabling the threshold power to be 344  $\mu$ W. The work demonstrated in the chalcogenide microresonator is important for the potential applications of chalcogenide glass, which has higher nonlinearity and low absorptions at mid-infrared band.

**Index Terms**—Microsphere, Brillouin scattering, chalcogenide glass.

## I. INTRODUCTION

STIMULATED Brillouin scattering (SBS) is a non-linear acoustic/optical phenomenon resulting from the interaction between an electromagnetic (optical) wave and a mechanical

(acoustic) wave, first proposed by Brillouin in 1922 [1]. Electrostriction occurs in the medium due to the presence of the pump light, and the resulting generated acoustic field then scatters the incident light at optical frequencies red-shifted or blue-shifted to generate a Stokes or an anti-Stokes optical signal. The beat frequency between the scattered and incident signals is the acoustic frequency. SBS is widely used in ultra-narrow linewidth lasers, distributed sensors, optical amplifiers, optical cooling, slow light, optical isolator, non-reciprocal optics and optical phase conjugation [2]–[11]. Specifically, SBS has also been realized in optical microresonators, such as silica microspheres, disks, microbottles, crystalline cylinders and nanoparticles [7], [12]–[16], in which the optical and acoustic waves circulate along the equatorial surface, forming optical and mechanical whispering-gallery modes (WGMs) with ultrahigh quality ( $Q$ ) factors.

The SBS process can become triply resonant when the pump, the Stokes/anti-Stokes and the acoustic waves are all resonant with the relevant optical and mechanical modes. These three fields therefore satisfy the conservation of energy and momentum in the microcavity. To date SBS in WGM microcavity was predominantly investigated utilizing silica [17], [18] and crystal resonators [13], or silicone oil droplets [19], [20]. However, the use of microspheres made from chalcogenide glasses, initially investigated 60 years ago [21], allows to study SBS in the mid-infrared region, as well as to exploit the relatively strong nonlinear optical characteristics of this materials. Chalcogenides are mainly composed of group VIA elements (excluding oxygen) in the periodic table, which results in their unique property of relatively high transmission in the infrared region, as well as suitability to form integrated waveguide optics and optical fibers in this spectral region [22], [23]. In addition, their phonon energy is extremely low compared to quartz, thus facilitating relatively easy fabrication of mid-infrared lasers, generally achieved by doping the chalcogenide glass with rare earth ions [21]. The use of chalcogenide glass microresonators reported in the literature has so far been confined mainly to temperature sensing [24], integrated waveguide devices and Raman scattering [22], [23], [25]. It should be noted that the chalcogenide glass purity is crucial to the successful fabrication of microresonators. The presence of oxygen and hydrocarbon results in a significant absorption peak in the near-/mid-infrared spectral regions [5], [26].

In this work, a high purity chalcogenide glass fiber has been used to obtain compound chalcogenide microspheres with a

Manuscript received December 2, 2021; revised January 14, 2022; accepted January 19, 2022. Date of publication January 25, 2022; date of current version January 27, 2022. This work was supported in part by the National Natural Science Foundation of China under Grants 61935006, 62005060, 61905048, 62090062, and 61805074, in part by the National Key Research and Development Program of China under Grant 2020YFA0607602, in part by the Shenzhen Technical Project under Grant JCYJ20190808173619062, in part by the 111 project to the Harbin Engineering University under Grant B13015, and in part by the Heilongjiang Touyan Innovation Team Program. (Corresponding author: Pengfei Wang.)

Jibo Yu and Yuxuan Jiang are with the Key Laboratory of In-fiber Integrated Optics of Ministry of Education College of Physics and Optoelectronic Engineering, Harbin Engineering University, Harbin 150001, China (e-mail: yu20131164@hrbeu.edu.cn; merak@hrbeu.edu.cn).

Zhen Shen and Chun-Hua Dong are with the Key Laboratory of Quantum Information, University of Science and Technology of China, Hefei 230026, China, and also with the Synergetic Innovation Center of Quantum Information and Quantum Physics, University of Science and Technology of China, Hefei 230026, China (e-mail: shenzhen@ustc.edu.cn; chunhua@ustc.edu.cn).

Zhiyong Yang and Sisheng Qi are with the Jiangsu Key Laboratory of Advanced Laser Materials and Devices School of Physics and Electronic Engineering, Jiangsu Normal University, Xuzhou, Jiangsu 221116, China (e-mail: yangzhiyong@jsnu.edu.cn; 1243725293@qq.com).

Gilberto Brambilla is with the Optoelectronics Research Centre, University of Southampton, Southampton SO17 1BJ, U.K. (e-mail: gb2@orc.soton.ac.uk).

Pengfei Wang is with the Key Laboratory of In-Fiber Integrated Optics of Ministry of Education, College of Science Harbin Engineering University, Harbin 150001, China, and also with the Key Laboratory of Optoelectronic Devices and Systems of Ministry of Education and Guangdong Province College of Optoelectronic Engineering, Shenzhen University, Shenzhen 518060, China (e-mail: pengfei.wang@tudublin.ie).

Digital Object Identifier 10.1109/JPHOT.2022.3145033

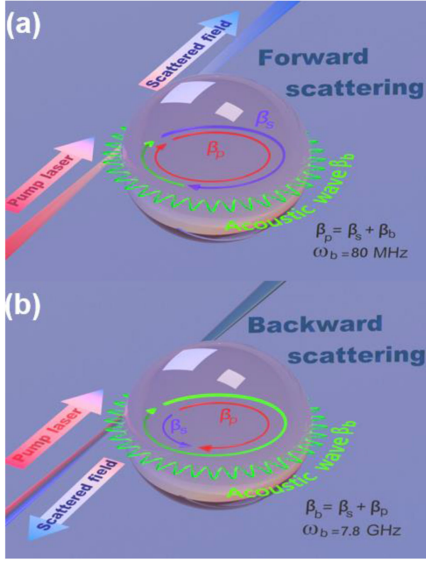


Fig. 1. The interaction of pump light (red), acoustic field (green) and scattered light (blue) in the microsphere with forward (a) and backward (b) scattering SBS, respectively. And the arrows represent the momentum conservation between the pump laser, Stokes signal and acoustic wave in chalcogenide glass for different SBS process.

quality factor as high as  $2.1 \times 10^7$ . In the case of the microresonators of this investigation, an opto-mechanical phenomenon induced by SBS has been observed for the first time. The threshold power of the backward SBS was measured to be as low as  $344 \mu\text{W}$ . This optomechanical phenomenon in chalcogenide microspheres can be exploited to realize non-reciprocal photonics devices, light storage, wavelength conversion, especially in the mid-infrared region, analogue to electro-optics and optomechanical systems [8], [9], [18], [27], [28].

## II. NUMERICAL SIMULATION OF OPTICAL AND MECHANICAL MODES

SBS originates from the interaction between the electric and the acoustic fields in chalcogenide microspheres, i.e., the interaction between photons and acoustic phonons. In the work presented in this article, SBS generation is due to the influence of the electric field of the propagating optical wave on the electrostriction of the chalcogenide medium. So that the variation of the period density and the dielectric constant occurring within the microsphere are accompanied by the generation of the acoustic field, resulting in coherent light scattering between the pump light and the acoustic field. A schematic diagram field, as shown in Fig. 1 below.

The fundamental condition for SBS generation in the microsphere requires that energy and momentum conservation is obeyed [29]. In this case the energy conservation requires  $\omega_p = \omega_s + \omega_b$ , while momentum conservation requires  $\beta_p = \beta_s + \beta_b$ , where  $\omega_p$ ,  $\omega_s$  and  $\omega_b$  are the angular frequency of the pump, Stokes, and acoustic signals respectively, while  $\beta_p$ ,  $\beta_s$  and  $\beta_b$  are the corresponding propagation constants.

According to the condition of momentum conservation matching between the pump signal, acoustic signal and Stokes signal, the SBS is divided into forward and backward SBS. These

are shown schematically in Fig. 1. In the experiment of this investigation, the microcavity comprises the chalcogenide glass microsphere with a diameter of  $70 \mu\text{m}$ , and then a tunable laser with the wavelength of  $1.55 \mu\text{m}$  resulted in an acoustic frequency  $\omega_b$  of 80 MHz and 7.8 GHz for forward and backward Brillouin scattering, respectively.

In the process of generating SBS, the pump signal, the Stokes signal and the acoustic signal need to simultaneously support the occurrence of resonance in the microsphere, resulting in integer azimuthal mode numbers [14]. If the azimuthal mode number of the pump and Stokes signals are  $m_p$  and  $m_s$  respectively, and the frequency of the acoustic wave is several orders of magnitude smaller than the light signal, it is reasonable to assume  $m_p \approx m_s$ . According to the formula of the resonant frequency in the microsphere [30], an azimuth mode number  $m_p \approx m_s \approx 333$  and the first order radial order can be used to separately satisfy the radial and azimuthal conditions. The azimuth number of the acoustic signal  $m_b$  indicates the number of mechanical modes that propagate inside the microsphere, which satisfy the following condition:

$$m_b = \frac{2\pi r \omega_b}{V}. \quad (1)$$

where  $V$  is the propagation speed of sound in chalcogenide glass,  $V \approx 2200 \text{ ms}^{-1}$ . As the acoustic frequency generated by forward SBS is 80 MHz, the forward mode number  $m_b$  is calculated to be 8, and according to the momentum conservation in the microsphere,  $m_p = m_s + m_b$ , the earlier assumption that  $m_p \approx m_s$  is thus validated.

If the polar direction is not considered in the microsphere, the formula of the resonant frequency is simplified to obtain [31]:

$$\beta_k \cong \frac{1}{r} \left[ m_k + \alpha_{n_k} \left( \frac{m_k}{2} \right)^{1/3} - \frac{1}{n_0 \sqrt{n_0^2 - 1}} \right]. \quad (2)$$

where  $k$  represents p or s,  $n_p$  and  $n_s$  are radial order of the pump and Stokes light, respectively,  $\alpha$  represents the Airy function and  $r$  represents the radius of microsphere. The radial relationship between the pump and Stokes signals in the forward SBS is:

$$m_b = \left[ (\alpha_{n_s} - \alpha_{n_p}) \left( \frac{m_s}{2} \right)^{1/3} \right]. \quad (3)$$

Substituting the values of  $m_b = 8$ ,  $m_s = 333$  and  $n_0 = 2.435$  into equation (2), when the Stokes light is in the first-order radial direction  $n_s = 1$ , the solution of the equation  $\alpha_{n_s} - \alpha_{n_p}$  cannot be obtained as in reference [20]. By increasing  $n_s$  to 2,  $m_s$  is changed to 322 [30], and equation (3) is satisfied when  $n_p$  is 3. This indicates that the momentum conservation of forward SBS can be achieved based on coupling between the two different high radial adjacent optical modes. The acoustic mode field pattern in the chalcogenide glass microsphere was calculated using the frequency domain and solid mechanics modules in the commercial software COMSOL Multiphysics, thus obtaining a radial mode distribution as described in the reference [17], [32]. An acoustic mode with a frequency of 80 MHz is shown in Fig. 4. Since the azimuth number  $m_b$  is 8, only the rotating body with an angle of  $\theta = 360/m_b$  degrees is shown in this case. In the simulations, the following parameters were used: Young's module  $E = 16 \text{ GPa}$ , refractive index  $n_0 = 2.435$ , density  $\rho_s =$

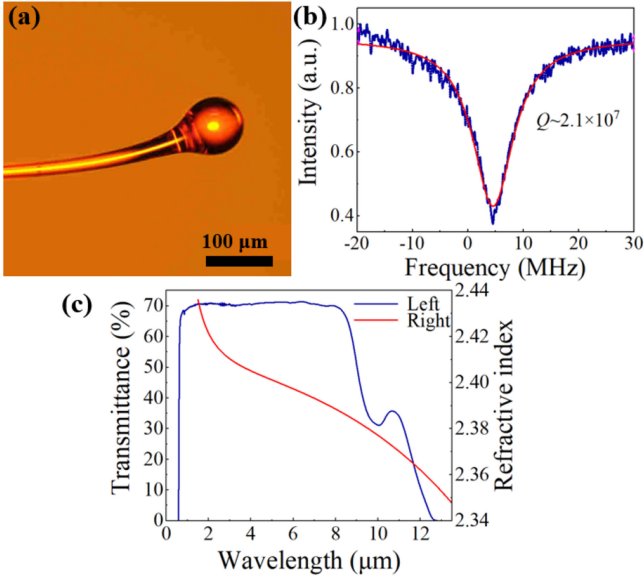


Fig. 2. (a) Microscope image of chalcogenide microsphere. (b) Typical WGM resonance spectrum of the chalcogenide glass microsphere with Lorentz fitting (red line), corresponding to the loaded  $Q$  of  $2.1 \times 10^7$ . (c) Blue: Transmission spectrum of the chalcogenide glass; Red: Dispersion curve of chalcogenide glass.

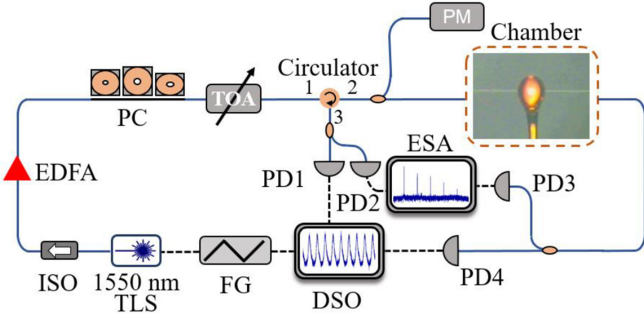


Fig. 3. Experimental setup for the measurement of forward and backward SBS in the chalcogenide glass microsphere. The green line represents the optical path, while black dash lines are the electrical connections. FG, function generator; EDFA, erbium doped fiber amplifier; ISO, isolator; PC, polarization controller; TOA, tunable optical attenuator; OC, optical coupler; ESA, electrical spectrum analyzer; PD, photo detector; PM, power meter.

$3200 \text{ kg m}^{-3}$ , Poisson's ratio  $\nu_s = 0.305$ , speed of sound  $V = 2200 \text{ ms}^{-1}$  and diameter  $D = 70 \text{ } \mu\text{m}$ .

### III. CHALCOGENIDE GLASS MICROSPHERE

The chalcogenide microsphere was fabricated from a bulk  $\text{As}_{0.39}\text{S}_{0.61}$  glass, synthesized by melting a mixture of 6N-purity sulfur and 7N-purity arsenic in a flamed-sealed low-OH quartz tube with an internal vacuum pressure of  $<10^{-3} \text{ Pa}$ . The sulfur particles were pre-sublimated 4 times under vacuum to eliminate carbon and S-H impurities, and the arsenic lumps were preheated under vacuum at  $210 \text{ }^\circ\text{C}$  for 1 hour to remove the volatile oxide impurities which resulted in high-purity glass. To further improve the glass purity, a chemical distillation technique was applied. Ultra-dry  $\text{GaCl}_3$  (5N-purity) and Al (5N-purity) were used as the C/H scavenging agent and oxygen getter, respectively. The detailed description of the fabrication process is included in reference [33]. At the final stage, the compound

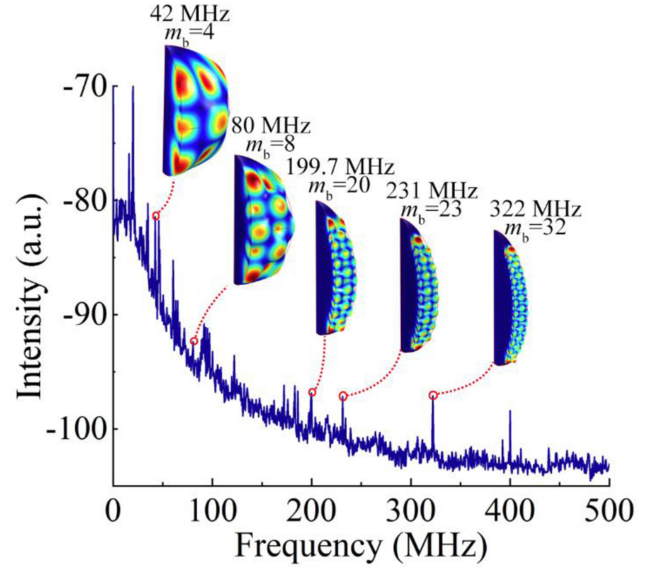


Fig. 4. Many mechanical modes are observed when the pump laser is scanned slowly from 1530 to 1620 nm at low power. The deformation patterns are the theoretical simulation of the mechanical modes that satisfy the resonant frequencies, and the rotating body with an angle of  $\theta = 360/m_b$  degrees is shown here.

in the quartz tube was rehomogenized at  $800 \text{ }^\circ\text{C}$  for about 12 hours in a rocking furnace, and the furnace temperature was then lowered to  $450 \text{ }^\circ\text{C}$ . The tube containing the melt was finally quenched in water and the formed glass was annealed at  $195 \text{ }^\circ\text{C}$  for 3 hours. Two discs were cut from the glass rod ( $15 \text{ mm}$  diameter  $\times$   $100 \text{ mm}$  height) for optical quality assessment. The remaining part was drawn into coreless fibers with a diameter of  $\sim 300 \text{ } \mu\text{m}$  using a dedicated in-house constructed drawing tower.

The prepared chalcogenide fiber was then mounted vertically on a three-axis displacement stage, and a weight was attached at the bottom. A tapered fiber with a diameter of  $20 \text{ } \mu\text{m}$  was fabricated using a  $\text{CO}_2$  laser. However, chalcogenide glasses have relatively high transmittance in the mid-infrared wavelength region and absorb less power after being drawn, which makes it impossible to continue heating the end of the tapered fiber to form microspheres using a  $\text{CO}_2$  laser. The prepared half tapered chalcogenide fiber was thus placed close to a ceramic heater operated at  $300 \text{ }^\circ\text{C}$ , which is higher than the softening temperature of the chalcogenide glass. Finally, the chalcogenide microsphere was formed due to surface tension [34], [35]. Fig. 2(a) shows the typical image of the fabricated chalcogenide microsphere.

The transmission spectrum of the glass was recorded on a double-side polished disc using a PerkinElmer Lambda 950 spectrophotometer in the  $0.5\text{--}3 \text{ } \mu\text{m}$  range, and a Fourier transform infrared (FTIR) spectrophotometer (Bruker Tensor 27) for the  $3\text{--}20 \text{ } \mu\text{m}$  region, as shown in Fig. 2(c). And the refractive indices of the glass in the  $1.7\text{--}20 \text{ } \mu\text{m}$  spectral range were also measured using a J. A. Woollam infrared variable angle spectroscopic ellipsometer. The measurement details are reported in reference [36]. The transmission loss of the fibers was measured using the cut-back method. A  $1.55 \text{ } \mu\text{m}$  continuous wave (CW) laser diode and an InGaAs detector were used to perform the measurement and the resulting loss was found to be  $0.86 \text{ dB m}^{-1}$ .

#### IV. STIMULATED MECHANICAL VIBRATION

To characterize the fabricated 70  $\mu\text{m}$  chalcogenide glass microsphere, the experimental setup is shown in Fig. 3. A tunable laser operating around the wavelength of 1550 nm was coupled into the microresonator through a tapered fiber, and the diameter was controlled to be  $\sim 1.5 \mu\text{m}$ . A fiber polarization controller (PC) was used to control the polarization of the input beam. A fraction of the output light was monitored using a low noise photo-detector (PD1&4) and digital oscilloscope (DSO). The remaining output light was measured by the high frequency detector (PD2&3, 25 GHz) and electrical spectrum analyzer.

First of all, the optical modes of the chalcogenide glass microsphere were studied by fine scanning the frequency of the tunable laser, as shown in Fig. 2(b). It should be noted that the power of the laser in the experiment was kept low, to avoid resonance broadening due to thermal effects within the microsphere during the frequency up-scanning process [37]. The loaded  $Q$  factor of the chalcogenide microsphere was calculated as being circa  $2.1 \times 10^7$ , which is very close to the theoretical absorption-limited  $Q$  factor [38] of  $5 \times 10^7$ , and we can also infer that it has a high  $Q$  value in the mid-infrared region.

To study the stimulated mechanical vibration by the forward or backward SBS of the chalcogenide glass microsphere, the forward acoustic signal and transmission of the microsphere were detected using PD3 and PD4, and the remaining PD1 and PD2 were used to measure the backward signal through the circulator. The mechanical modes shown in Fig. 4.

It was observed by slowly scanning the tunable laser (TL) from 1520-1630 nm. The recorded mechanical frequency range was set to 0-500 MHz. The theoretical simulation is in good agreement with the corresponding measured resonant frequency of the mechanical modes, as described in the previous section on numerical simulation.

The signal at the frequency of 80 MHz in Fig. 5. represents the beat frequency between the pump and the Stokes signals, and no cascaded signals were observed on the ESA. A tunable Fabry–Pérot (FP) spectrum analyzer (Thorlabs SA200-14A) was used to verify that the mechanical vibration was generated by the Stokes signal. The inset in Fig. 5(a) shows that the mechanical linewidth measured at a low pump power is about 170 KHz. In addition, there is a breath mode induced by light pressure at the peak of  $\sim 20$  MHz.

On the other hand, the backward SBS of the chalcogenide glass microsphere was observed using the ESA via the circulator in the optical path. The beat signal was generated by the interaction of the backscattered pump signal with the Stokes signal, and a portion of the pump signal was additionally introduced to amplify the beat signal. The radio frequency spectrum measured in the experiment is shown in Fig. 5(c). The result shows that a beat signal with a frequency of 7.82 GHz is generated.

Finally, the threshold of the optomechanical vibration generated by backward SBS was experimentally determined. The pump laser is thermally locked at the optical mode due to the high  $Q$  chalcogenide glass microresonator possess stronger thermal effect. When the pump power coupled to the microsphere was changed, the resonant wavelength was shifted by a few picometers. The pump power in the microsphere is calculated through

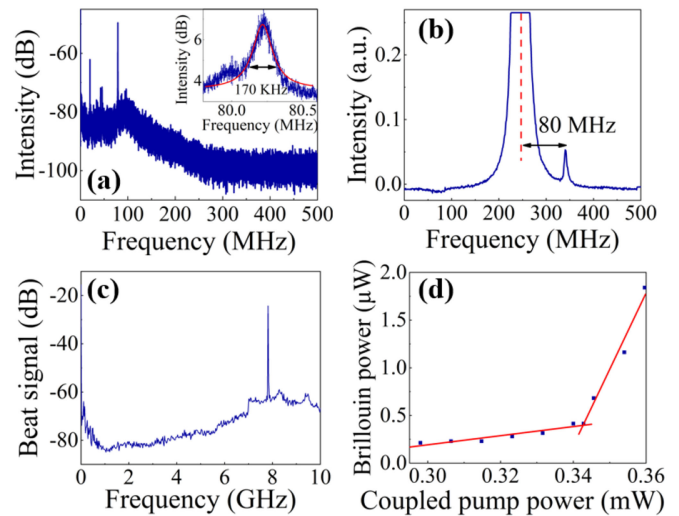


Fig. 5. (a) Frequency domain diagram of forward acoustic signal; the inset shows the mechanical linewidth, which is about 170 KHz at low input pump power. (b) A single sideband with a frequency of 80 MHz was detected using FP interferometer. (c) Radio frequency spectrum of the chalcogenide glass microsphere induced by the backward Brillouin, in which the frequency is 7.82 GHz. (d) Relationship between the coupled pump power and the backward Stokes power, where the threshold is 344  $\mu\text{W}$ .

monitoring the transmission on the DSO. Fig. 5(d) shows that the oscillation threshold was 344  $\mu\text{W}$ . This point indicates that the mechanical mode in the microcavity is optically excited, and the acoustic signal is amplified to be larger than the loss of the material. Moreover, when the coupled pump power exceeds the threshold, the conversion efficiency of the Stokes light is 7.72%.

#### V. CONCLUSION

In conclusion, a high-purity compound chalcogenide glass microsphere has been successfully fabricated, and its optomechanical behavior induced by SBS in the microcavity has been studied. In the theoretical simulation, the mode field of the pump, Stokes and acoustic waves were calculated when the phase-matched triply resonant interaction was satisfied. The microsphere was pumped using a TL in the band of 1550 nm which yielded a  $Q$  value of  $2.1 \times 10^7$ . The beat signal generated by the interaction between the pump signal and forward SBS was 80 MHz, while the backward signal was 7.82 GHz. In addition, the threshold of the backward SBS in the microsphere was measured by changing the coupled pumped power, and was measured to be 344  $\mu\text{W}$ . This research could have a major impact on optomechanics in integrated chalcogenide waveguides, non-linearity in chalcogenide microcavities, and general investigation of SBS phenomena in the mid-infrared.

#### REFERENCES

- [1] L. Brillouin, "Diffusion de la lumière et des rayons X par un corps transparent homogène," *Ann. Phys.*, vol. 9, no. 17, pp. 88–122, 1922.
- [2] W. T. Whitney, M. T. Duignan, and B. J. Feldman, "Stimulated Brillouin scattering phase conjugation of an amplified hydrogen fluoride laser beam," *Appl. Opt.*, vol. 31, no. 6, pp. 699–702, 1992.

- [3] V. I. Kovalev and R. G. Harrison, "Suppression of stimulated Brillouin scattering in high-power single-frequency fiber amplifiers," *Opt. Lett.*, vol. 31, no. 2, pp. 161–163, 2006.
- [4] M. G. Herráez, K. Y. Song, and L. Thévenaz, "Arbitrary-bandwidth Brillouin slow light in optical fibers," *Opt. Exp.*, vol. 14, no. 4, pp. 1395–1400, 2006.
- [5] B. J. Eggleton, B. Luther-Davies, and K. Richardson, "Chalcogenide photonics," *Nature Photon.*, vol. 5, pp. 141–148, Feb. 2011.
- [6] G. Bahl, M. Tomes, F. Marquardt, and T. Carmon, "Observation of spontaneous Brillouin cooling," *Nature Phys.*, vol. 8, no. 3, pp. 203–207, 2012.
- [7] W. Loh *et al.*, "Dual-microcavity narrow-linewidth Brillouin laser," *Optica*, vol. 2, no. 3, pp. 225–232, 2015.
- [8] C. H. Dong, Z. Shen, C. L. Zou, Y. L. Zhang, W. Fu, and G. C. Guo, "Brillouin-scattering-induced transparency and non-reciprocal light storage," *Nature Commun.*, vol. 6, pp. 2–7, 2015.
- [9] J. Kim, M. C. Kuzyk, K. Han, H. Wang, and G. Bahl, "Non-reciprocal Brillouin scattering induced transparency," *Nature Phys.*, vol. 11, no. 3, pp. 275–280, 2015.
- [10] D. M. Chow, Z. Yang, M. A. Soto, and L. Thévenaz, "Distributed forward Brillouin sensor based on local light phase recovery," *Nat. Commun.*, vol. 9, no. 1, 2018, Art. no. 2990.
- [11] J. Ma *et al.*, "Chip-based optical isolator and nonreciprocal parity-time symmetry induced by stimulated Brillouin scattering," *Laser Photon. Rev.*, vol. 14, no. 5, 2020, Art. no. 1900278.
- [12] Y. Li *et al.*, "Micro-Brillouin scattering from a single isolated nanosphere," *Appl. Phys. Lett.*, vol. 88, no. 2, 2006, Art. no. 23112.
- [13] I. S. Grudin, A. B. Matsko, and L. Maleki, "Brillouin lasing with a CaF<sub>2</sub> whispering gallery mode resonator," *Phys. Rev. Lett.*, vol. 102, no. 4, Jan. 2009, Art. no. 43902.
- [14] G. Bahl, J. Zehnpfennig, M. Tomes, and T. Carmon, "Stimulated optomechanical excitation of surface acoustic waves in a microdevice," *Nature Commun.*, vol. 2, no. 1, pp. 403–406, 2011.
- [15] J. Li, H. Lee, and K. J. Vahala, "Microwave synthesizer using an on-chip Brillouin oscillator," *Nature Commun.*, vol. 4, Jun. 2013, Art. no. 2097.
- [16] S. Zhu, B. Xiao, B. Jiang, L. Shi, and X. Zhang, "Tunable Brillouin and Raman microlasers using hybrid microbottle resonators," *Nanophotonics*, vol. 8, no. 5, pp. 931–940, 2019.
- [17] G. Bahl, X. Fan, and T. Carmon, "Acoustic whispering-gallery modes in optomechanical shells," *New J. Phys.*, vol. 14, no. 11, 2012, Art. no. 115026.
- [18] C. Dong, V. Fiore, M. C. Kuzyk, L. Tian, and H. Wang, "Optical wavelength conversion via optomechanical coupling in a silica resonator," *Ann. Phys.*, vol. 527, no. 1/2, pp. 100–106, 2015.
- [19] R. Dahan, L. L. Martin, and T. Carmon, "Droplet optomechanics," *Optica*, vol. 3, no. 2, pp. 175–178, 2016.
- [20] A. Giorgini *et al.*, "Stimulated Brillouin cavity optomechanics in liquid droplets," *Phys. Rev. Lett.*, vol. 120, no. 7, 2018, Art. no. 73902.
- [21] R. Frerichs, "New optical glasses with good transparency in the infrared," *J. Opt. Soc. Amer.*, vol. 43, no. 12, pp. 1153–1157, 1953.
- [22] L. Li *et al.*, "Integrated flexible chalcogenide glass photonic devices," *Nature Photon.*, vol. 8, no. 8, pp. 643–649, 2014.
- [23] H. Lin *et al.*, "Chalcogenide glass-on-graphene photonics," *Nature Photon.*, vol. 11, no. 12, pp. 798–805, 2017.
- [24] Z. Yang, Y. Wu, X. Zhang, W. Zhang, P. Xu, and S. Dai, "Low temperature fabrication of chalcogenide microsphere resonators for thermal sensing," *IEEE Photon. Technol. Lett.*, vol. 29, no. 1, pp. 66–69, Jan. 2017.
- [25] T. Cheng *et al.*, "Mid-infrared cascaded stimulated Raman scattering up to eighth orders in As-S optical fiber," *Opt. Exp.*, vol. 26, no. 9, pp. 12007–12015, 2018.
- [26] S. Susman, S. Clark Rowland, and K. J. Volin, "The purification of elemental sulfur," *J. Mater. Res.*, vol. 7, no. 6, pp. 1526–1533, 1992.
- [27] V. Fiore, Y. Yang, M. C. Kuzyk, R. Barbour, L. Tian, and H. Wang, "Storing optical information as a mechanical excitation in a silica optomechanical resonator," *Phys. Rev. Lett.*, vol. 107, no. 13, 2011, Art. no. 133601.
- [28] J. T. Hill, A. H. Safavi-Naeini, J. Chan, and O. Painter, "Coherent optical wavelength conversion via cavity optomechanics," *Nature Commun.*, vol. 3, no. 1, 2012, Art. no. 1196.
- [29] N. Dostart, S. Kim, and G. Bahl, "Giant gain enhancement in surface-confined resonant stimulated Brillouin scattering," *Laser Photon. Rev.*, vol. 9, no. 6, pp. 689–705, 2015.
- [30] S. Schiller, "Asymptotic expansion of morphological resonance frequencies in Mie scattering," *Appl. Opt.*, vol. 32, no. 12, pp. 2181–2185, 1993.
- [31] A. B. Matsko, A. A. Savchenkov, V. S. Ilchenko, D. Seidel, and L. Maleki, "Optomechanics with surface-acoustic-wave whispering-gallery modes," *Phys. Rev. Lett.*, vol. 103, no. 25, 2009, Art. no. 257403.
- [32] J. Zehnpfennig, G. Bahl, M. Tomes, and T. Carmon, "Surface optomechanics: Calculating optically excited acoustical whispering gallery modes in microspheres," *Opt. Exp.*, vol. 19, no. 15, pp. 14240–14248, 2011.
- [33] B. Zhang *et al.*, "Low loss, high NA chalcogenide glass fibers for broadband mid-infrared supercontinuum generation," *J. Amer. Ceram. Soc.*, vol. 98, no. 5, pp. 1389–1392, 2015.
- [34] Y.-F. Xiao, C.-H. Dong, Z.-F. Han, and G.-C. Guo, "Directional escape from a high- $Q$  deformed microsphere induced by short CO<sub>2</sub> laser pulses," *Opt. Lett.*, vol. 32, no. 6, pp. 644–646, 2007.
- [35] P. Wang *et al.*, "Chalcogenide microsphere fabricated from fiber tapers using contact with a high-temperature ceramic surface," *IEEE Photon. Technol. Lett.*, vol. 24, no. 13, pp. 1103–1105, Jul. 2012.
- [36] Y. Yang *et al.*, "Composition dependence of physical and optical properties in Ge-As-S chalcogenide glasses," *J. Non-Crystalline Solids*, vol. 440, pp. 38–42, 2016.
- [37] T. Carmon, Lan Yang, and K. J. Vahala, "Dynamical thermal behavior and thermal self-stability of microcavities," *Opt. Exp.*, vol. 12, no. 20, pp. 2019–2021, 2004.
- [38] M. L. Gorodetsky, A. A. Savchenkov, and V. S. Ilchenko, "Ultimate  $Q$  of optical microsphere resonators," *Opt. Lett.*, vol. 21, no. 7, pp. 453–455, 1996.